Polym. Korea, Vol. 49, No. 5, pp. 556-563 (2025)
https://doi.org/10.7317/pk.2025.49.5.556
ISSN 2234-8077(Online)

유기태양전지를 위한 새로운 빌딩블록인 Pyridoquinolinedione와 고분자 도너의 합성

이수하 · 곽선이 · 박혜정* · 황도훈†
부산대학교 화학과, *창원대학교 생물화학융합학부
(2025년 1월 13일 접수, 2025년 4월 8일 수정, 2025년 4월 9일 채택)

Pyridoquinolinedione as a New Building Block for Semiconducting Polymer Donors in Organic Solar Cells

Suha Lee, Seon Lee Kwak, Hea Jung Park* and Do-Hoon Hwang†
Department of Chemistry and Chemistry Institute for Functional Materials, Pusan National University, Busan 46241, Korea
**Department of Biology and Chemistry, Changwon National University, Changwon 51140, Korea*
(Received January 13, 2025; Revised April 8, 2025; Accepted April 9, 2025)

초록: 본 연구에서는 새로운 다환 락탐 구조를 가지는 pyrido[2,3-g]quinoline-2,7(1*H*,6*H*)-dione(PQD)를 설계 합성하였고 이를 benzodithiophene(BDT) 유도체와 중합하여 두 종의 새로운 반도체성 고분자인 PPQD-BDT와 PPQDT-BDT를 Stille 중합을 통하여 합성하였다. 락탐 고리는 약하게 전자를 당기는 특징을 가지고 있어 BDT 유도체와 같은 도너와 중합할 경우 밴드 갭이 비교적 큰 반도체 고분자를 합성할 수 있다. 최근에 개발된 유기태양전지용 억셉터 재료들은 장파장 영역에 흡수를 가지고 있어 도너 고분자는 상대적으로 단파장 영역에서 흡수할 수 있는 밴드 갭이 큰 고분자가 광활성 층으로 유리하다. 합성된 PPQD-BDT와 PPQDT-BDT는 밴드 갭이 각각 1.93과 1.85 eV 였다. 유기태양전지 능력을 평가하기 위해 ITIC와 Y6를 억셉터로 사용한 유기태양전지를 제작하였으며 PPQDT-BDT의 경우 Y6와 함께 광활성 층으로 사용하였을 때 최대 전력변환효율 4.52%의 광전변환 효율을 보였다. 본 연구에서 합성된 PQD 단량체는 BDT 이외의 다양한 공단량체들과 공중합이 가능하여 구조의 최적화를 통하여 유기태양전지, 유기트랜지스터, 유기광검출기 등의 전자 소자에 활용될 수 있을 것으로 기대된다.

Abstract: The molecular design strategy of alternating electron donor and acceptor units is widely used to develop polymer donors for organic solar cells (OSCs), enabling tuning of absorption spectra and frontier molecular orbital energies. To enhance the efficiency and stability of OSCs, researchers have created new materials with novel donor and acceptor units. In this study, pyrido[2,3-g]quinoline-2,7(1*H*,6*H*)-dione (PQD) was introduced as a new polycyclic lactam building block. The synthesized polymers, PPQD-BDT and PPQDT-BDT, exhibited broad absorption from 300 to 700 nm and a wide bandgap of 1.93 and 1.85 eV, respectively. OSC devices were fabricated using these polymers as donors blended with a non-fullerene acceptor (ITIC). The maximum power conversion efficiency (PCE) of PPQDT-BDT was 2.86% due to better molecular orientation in the film state, whereas PPQD-BDT exhibited a lower PCE of 1.34%. Moreover, OSC devices based on PPQDT-BDT blended with Y6 as a non-fullerene acceptor showed a PCE of 4.52%.

Keywords: organic solar cell, polycyclic building block, lactam, polymer donor.

Introduction[a]

Bulk heterojunction (BHJ) organic solar cells (OSCs) have been attracting research interest for the last few decades because of their light weight, flexibility, low production cost, and tunable light absorption range.[1-6] The power conversion efficiency (PCE) of single-junction BHJ OSC has increased to over 18%, due to enormous efforts in the development and synthesis of new photoactive materials such as donors and acceptors and the optimization of device configurations.[7-9] However, the PCE and stability of OSCs are still lower than those of Si-based solar cells. Therefore, continuous development of new photoactive materials is required to improve the stability and performance of OSCs.

In donor(D)-acceptor(A) type conjugated copolymers, electron donor and acceptor units are alternately connected to tune

†To whom correspondence should be addressed.
dohoonhwang@pusan.ac.kr, ORCID 0000-0003-4183-0185

the absorption spectra and frontier molecular orbital (FMO) energies.[10-13] Benzodithiophene (BDT) is a popular donor unit in the OSC field, because its planar structure can lead to high hole mobility[14] and preferential face-on molecular orientation, which are advantageous for organic photovoltaics (OPV) based on polymer thin films.[15] Several electron-withdrawing units have been combined with the BDT unit by copolymerization, and the resultant copolymers exhibited high photovoltaic performance.[16] However, there is still a need for novel OSC active layer materials with higher photovoltaic performance.

Among the electron-withdrawing units, polycyclic aromatic lactams have shown promise as efficient donor materials in D-A copolymers.[17-19] For example, thiophene-substituted diketopyrrolopyrrole (DPPT), isoindigo (IID), and thieno[3,4-*c*]pyrrole-4,6-dione (TPD) have been considered desirable electron-withdrawing building blocks owing to the lactam moieties in their molecular structures. The lactam moiety has a high electron affinity and a quasi-planar backbone, and the solubility can be easily controlled by introducing appropriate alkyl or aryl groups at the N-position of this moiety.[20] Recently, Yoon *et al*. developed a new bis-lactam-based electron-deficient unit, 3,7-dithiophene-2-yl-dialkyl-1,5-naphthyridine-2,6-dione (NTDT), which has a larger ring size compared to DPPT. They successfully synthesized a polymer donor P(NTDT-BDT) consisting of electron-accepting NTDT and electron-donating BDT units. The corresponding device demonstrated PCE = 8.16% with V_{OC} = 0.70 V and J_{SC} = 18.51 mA cm^{-2}.[21]

In this study, we designed and synthesized a new lactam-based electron-withdrawing unit, pyrido[2,3-*g*]quinoline-2,7(1*H*,6*H*)-dione (PQD), consisting of a tricyclic aromatic lactam. The designed structure of PQD contains a phenyl between the two lactams of NTDT. Because of the expanded π-conjugation length, PQD can absorb in a wider wavelength range than NTDT, and the corresponding polymers have improved planarity owing to the fused tricyclic structure. Two D-A copolymers were successfully synthesized by combining PQD with BDT as an electron-donating unit, namely poly {3-(4,8-bis(5-(2-ethylhexyl)thiophen-2-yl)benzo[1,2-*b*:4,5-*b*']dithiophen-2-yl)-1,6-didodecylpyrido [2,3-*g*]quinoline-2,7(1*H*,6*H*)-dione} (PPQD-BDT) and poly {3-(5-(4,8-bis(5-(2-ethylhexyl)thiophen-2-yl)benzo[1,2-*b*:4,5-*b*']dithiophen-2-yl)-4-(2-ethylhexyl)thiophen-2-yl)-1,6-didodecyl-8-(4-(2-ethylhexyl)thiophen-2-yl)pyrido [2,3-*g*]quinoline-2,7(1*H*,6*H*)-dione} (PPQDT-BDT). These copolymers were characterized by their optical, electrochemical, and thermal properties. The systematic synthetic routes and molecular structures of the PQD building blocks and the corresponding polymers are shown in Scheme 1 and 2, respectively.

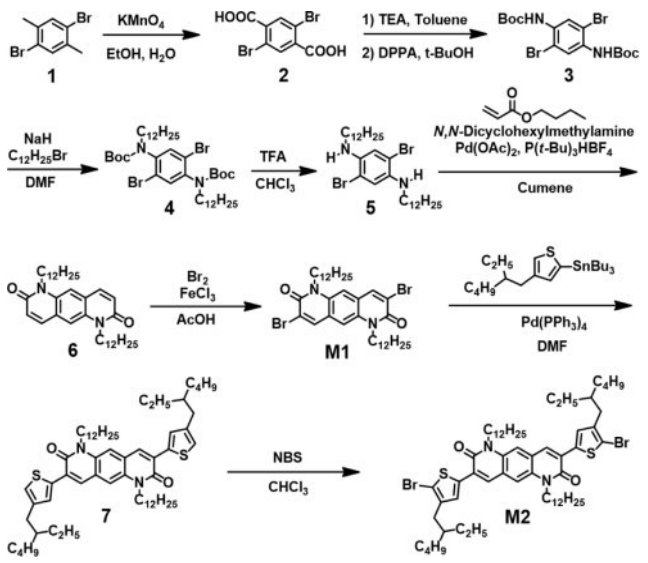

Scheme 1. Synthetic route to monomers **M1** and **M2**.

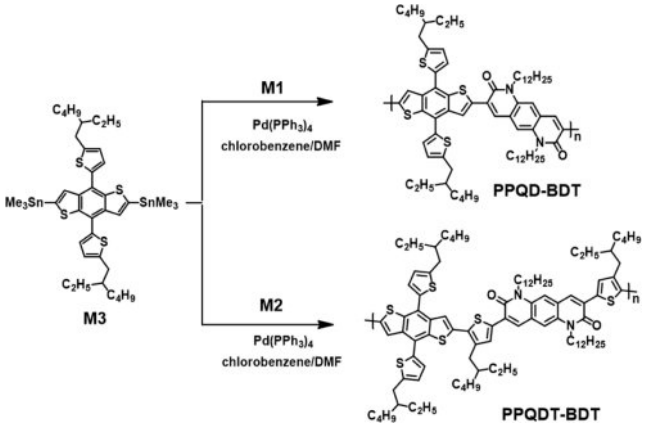

Scheme 2. Synthetic route to copolymers PPQD-BDT and PPQDT-BDT.

[a]Abbreviations: atomic force microscopy (AFM), benzodithiophene (BDT), bulk heterojunction (BHJ), chlorobenzene (CB), cyclic voltammetry (CV), density functional theory (DFT), differential scanning calorimetry (DSC), N,N-dimethylformamide (DMF), diphenyl ether (DPE), 3,7-dithiophene-2-yl-dialkyl-1,5-naphthyridine-2,6-dione (NTDT), external quantum efficiency (EQE), frontier molecular orbital (FMO), gel permeation chromatography (GPC), grazing incidence wide-angle X-ray scattering (GIWAXS), grazing-incidence X-ray diffraction (GIXD), in-plane (IP), indium tin oxide (ITO), isoindigo (IID), organic photovoltaics (OPV), organic solar cell (OSC), out-of-plane (OOP), poly {3-(4,8-bis(5-(2-ethylhexyl), thiophen-2-yl), benzo[1,2-*b*:4,5-*b*']dithiophen-2-yl), -1,6-didodecylpyrido [2,3-*g*]quinoline-2,7(1*H*,6*H*),-dione} (PPQD-BDT), poly {3-(5-(4,8-bis(5-(2-ethylhexyl), thiophen-2-yl), benzo[1,2-*b*:4,5-*b*']dithiophen-2-yl), -4-(2-ethylhexyl), thiophen-2-yl),-1,6-didodecyl-8-(4-(2-ethylhexyl), thiophen-2-yl), pyrido [2,3-*g*]quinoline-2,7(1*H*,6*H*),-dione} (PPQDT-BDT), polydispersity index (PDI), power conversion efficiency (PCE), pyrido[2,3-*g*]quinoline-2,7(1*H*,6*H*),-dione (PQD), root-mean square (RMS), tetrabutylammonium tetrafluoroborate ($TBABF_4$), thermogravimetric analysis (TGA), thieno[3,4-*c*]pyrrole-4,6-dione (TPD), thiophene-substituted diketopyrrolopyrrole (DPPT).

Experimental

General Measurements. ^{1}H and ^{13}C NMR spectra were measured using a Varian Mercury Plus 300 MHz NMR spectrometer, and the chemical shifts were recorded using chloroform-d and dimethyl sulfoxide-d_6 in units of part per million (ppm). The thermal analysis included thermogravimetric analysis (TGA; TGA Q500 V20.13 Build 39) and differential scanning calorimetry (DSC; DSC Q2000 V24.4 Build 116). UV-Vis absorption spectra were obtained using a JP/UV-1800 UV/Vis spectrometer. The electrochemical properties were analyzed by cyclic voltammetry (CV) using a CH Instruments electrochemical analyzer in a solution of 0.1 M tetrabutylammonium tetrafluoroborate ($TBABF_4$) in acetonitrile at a scan rate of 0.05 V/s. A Pt wire was used as the counter electrode, and $Ag/AgNO_3$ was used as the reference electrode. The OPV performance was measured using a McScience K201 LAB50 solar simulator. The current density-voltage (*J-V*) curves of the devices were measured under AM 1.5G light conditions. The light intensity was calibrated using a Si standard reference device (PV Measurements Inc.) calibrated at the National Renewable Energy Laboratory. External quantum efficiency (EQE) data were measured using a McScience K3100 EQX system. The EQE values were obtained as a function of wavelength in the range of 300–800 nm under a xenon short arc lamp as the light source, and calibration was performed using a Si photodiode. Two-dimensional grazing-incidence X-ray diffraction (2D-GIXD) experiments were performed at the 3C beamline of the Pohang Accelerator Laboratory (PAL), Republic of Korea. X-rays with a wavelength of 1.2296 Å (10.0831 keV) were used. The incident angle (0.13°) was chosen to allow complete penetration of X-rays into the polymer film. The surface morphologies of the polymer/ITIC blend thin films were analyzed using a VEECO Dimension 3100 instrument and the Nanoscope V (Version 7.0) program.

Materials. All starting materials and reagents were purchased from commercial sources (Aldrich or Alfa Aesar) unless indicated otherwise. All manipulations involving air-sensitive reagents were performed under a dry nitrogen atmosphere. **M3** was purchased from a commercial source.

Synthesis. Synthesis of 2,5-dibromoterephthalic acid (2): In a 500-mL round-bottom flask, 1,4-dibromoxylene (30.0 g, 0.114 mol) and potassium permanganate (39.5 g, 0.250 mol) were dissolved in a mixed solution of *t*-BuOH and H_2O (1:1 v/v, 300 mL) and then stirred at 100 ℃. After 1 h, more potassium permanganate (39.5 g, 0.250 mol) was added and refluxed at 100 ℃ for 12 h under stirring. The mixture was cooled to room temperature and passed through a celite filter. After removing the solvent under reduced pressure, the residue was stirred together with concentrated hydrochloric acid (12 M, 20 mL). The precipitate was then filtered under reduced pressure and washed with water. The obtained white solid was directly used in the next step. Product: 27.0 g (74%). ^{1}H NMR (300 MHz, $CDCl_3$, δ): 7.983 (2H, s).

Synthesis of di-tert-butyl(2,5-dibromo-1,4-phenylene) dicarbamate (3): In a 500 mL round-bottom flask, compound **2** (21.0 g, 0.0648 mol) and triethylamine (27.1 mL, 0.194 mol) were dissolved in *t*-BuOH (200mL) and stirred at 85 ℃ for 1 h. Subsequently, diphenyl phosphoryl azide (41.9 mL, 0.194 mol) was injected, followed by refluxing for 12 h. After cooling the reaction mixture to 0 ℃, the precipitate was filtered and washed with methanol. Product: 22.3 g (74%). ^{1}H NMR (300 MHz, $CDCl_3$, δ): 8.376 (2H, s), 6.874 (2H, s), 1.522 (18H, s).

Synthesis of 2,5-dibromo-*N*^{1},*N*^{4}-didodecylbenzene-1,4-diamine (5): Sodium hydride (60% dispersion in mineral oil, 2.57 g, 64.4 mmol) was suspended in anhydrous *N*,*N*-dimethylformamide (DMF, 20 mL) under N_2 condition. Compound **3** (10.00 g, 21.5 mmol) dissolved in DMF (80 mL) was added dropwise to the suspension of sodium hydride at 0 ℃. After 30 min, bromo-1-dodecane (15.5 mL, 64.4 mmol) was slowly added to the mixture and stirred at room temperature for 12 h. The mixture was poured into water to quench the residual sodium hydride and then extracted with dichloromethane. The solution was dried over $MgSO_4$, and the solvent was removed under reduced pressure. The residue was dissolved in a mixture of trifluoroacetic acid and chloroform (2:1 v/v, 30 mL) and stirred for 3 h. Residual trifluoroacetic acid was quenched using a saturated $NaHCO_3$ solution, followed by extraction with dichloromethane. After drying with $MgSO_4$, solvent in the extract was removed under reduced pressure. The residue was recrystallized in dichloromethane and methanol to afford a pale yellow solid (11.13 g, 86%). ^{1}H NMR (300 MHz, $CDCl_3$, δ): 6.790 (2H, s), 3.720 (2H, s), 3.037 (4H, t), 1.649 (4H, m), 1.364 (36H, m), 0.881 (6H, t).

Synthesis of 1,6-didodecylpyrido[2,3-*g*]quinoline-2,7(1*H*,6*H*)-dione (6): In a 250-mL round bottom flask, 2,5-dibromo-*N*^{1},*N*^{4}-didodecylbenzene-1,4-diamine (**4**) (5.00 g, 8.30 mmol), $Pd(OAc)_2$ (74.5 mg, 0.332 mmol), tri-*t*-butylphosphonium tetrafluoroborate (0.19 g, 0.664 mmol), *N*,*N*-dicyclohexylmethylamine (8.9 mL, 0.0415 mmol), and butyl acrylate (2.6 mL, 0.0183 mol) were dissolved in cumene (100 mL) and stirred at 150 ℃ for 12 h. The reaction mixture was cooled to 0 ℃, and the precipitate was filtered under reduced pressure to afford a yellow solid

(2.73 g, 60%). ^{1}H NMR (300 MHz, $CDCl_3$, δ): 7.754 (2H, d), 7.435 (2H, s), 6.810 (2H, s), 4.299 (4H, t), 1.761 (4H, m), 1.252 (36H, m), 0.873 (6H, t). ^{13}C NMR (100 MHz, $CDCl_3$, δ): 161.45, 138.19, 134.11, 124.18, 128.07, 113.4, 42.46, 31.92, 29.66, 29.63, 29.61, 29.57, 29.41, 29.35, 27.45, 27.03, 22.69, 14.13. HRMS(ESI) m/z calcd. for $C_{36}H_{56}N_2O_2$: 549.4415, found 549.4419 $[M + H]^+$.

Synthesis of 3,8-dibromo-1,6-didodecylpyrido[2,3-*g*]quinoline-2,7(1*H*,6*H*)-dione (**M1**): 1,6-Didodecylpyrido[2,3-*g*] quinoline-2,7(1*H*,6*H*)-dione (**6**) (2.73 g, 4.97 mmol) and iron (III) chloride (0.40 g, 2.49 mmol) were added to a 100-mL round-bottom flask and dissolved in acetic acid (50 mL). Bromine (5.1 mL, 99.5 mmol) was added dropwise and stirred at 100 ℃ for 24 h. The mixture was cooled to room temperature, and water was poured in to quench excess acetic acid. The precipitate was then filtered under reduced pressure and washed with methanol. The solid was recrystallized to afford a yellow-orange solid (3.34 g, 95%). ^{1}H NMR (300 MHz, $CDCl_3$, δ): 8.224 (2H, s), 7.257 (2H, s), 4.338 (4H, t), 1.766 (4H, m), 1.432 (36H, m), 0.883 (6H, t). ^{13}C NMR (100 MHz, $CDCl_3$, δ): 157.52, 139.69, 133.73, 122.86, 120.78, 112.48, 44.32, 31.92, 29.66, 29.64, 29.60, 29.54, 29.35, 27.34, 26.98, 22.70, 14.13. HRMS(ESI) m/z calcd. for $C_{36}H_{56}Br_2N_2O_2$: 705.2625, found 705.2617 $[M + H]^+$.

Synthesis of 1,6-didodecyl-3,8-bis(4-(2-ethylhexyl) thiophene-2-yl)pyrido[2,3-*g*]quinoline-2,7(1*H*,6*H*)-dione (7): Under N_2 atmosphere, 3,8-dibromo-1,6-didodecylpyrido[2,3-*g*]quinoline-2,7(1*H*,6*H*)-dione (**M1**) (2.00 g, 2.83 mmol), $Pd(PPh_3)_2Cl_2$ (0.12 g, 0.170 mmol), and tributyl(4-(2-ethylhexyl)thiophene-2-yl)stannane (4.12 g, 8.49 mmol) were dissolved in anhydrous DMF and stirred at 110 ℃ for 12 h. DMF was removed under reduced pressure. The mixture was purified using silica chromatography (dichloromethane:hexane = 1:1 as eluent) to afford a yellow solid (0.85 g, 32%). ^{1}H NMR (300 MHz, $CDCl_3$, δ): 8.131 (2H, s), 7.680 (2H, s), 7.488 (2H, s), 7.056 (2H, s), 4.408 (4H, t), 2.597 (4H, d), 1.841 (6H, m), 1.295 (48H, m), 0.892 (18H, m). ^{13}C NMR (100 MHz, $CDCl_3$, δ): 159.78, 141.97, 136.65, 133.11, 130.84, 128.12, 126.94, 124.80, 122.75, 112.36, 43.42, 40.44, 34.70, 32.52, 31.93, 29.67, 29.64, 29.50, 29.36, 28.93, 27.49, 27.22, 25.62, 23.10, 22.70, 14.18, 14.13, 10.86. HRMS(ESI) m/z calcd. for $C_{60}H_{92}N_2O_2S_2$: 936.6673, found 937.6678 $[M + H]^+$.

Synthesis of 3,8-bis(5-bromo-4-(2-ethylhexyl)thiophene-2-yl)-1,6-didodecylpyrido[2,3-*g*]quinoline-2,7(1*H*,6*H*)-dione (**M2**): In a 100-mL round-bottom flask, 1,6-didodecyl-3,8-bis(4-(2-ethylhexyl)thiophene-2-yl)pyrido[2,3-*g*]quinoline-2,7(1*H*,6*H*)-dione (**7**) (0.85 g, 0.91 mmol) was dissolved in chloroform. After cooling to 0 ℃, *N*-bromosuccinimide (0.48 g, 2.71 mmol) was added slowly in dark condition and stirred for 12 h. Water was poured into the mixture, followed by extraction with chloroform. The solvent was removed from the extract under reduced pressure using a rotary evaporator. The precipitate was purified using silica column chromatography (hexane: dichloromethane = 1:1 as eluent). The solid was recrystallized in isopropyl alcohol to afford a yellow solid (0.82 g, 83%). ^{1}H NMR (300 MHz, $CDCl_3$, δ): 8.130 (2H, s), 7.516 (2H, s), 7.469 (2H, s), 4.399 (4H, t), 2.556 (4H, d), 1.823 (6H, m), 1.299 (48H, m), 0.884 (18H, m). ^{13}C NMR (100 MHz, $CDCl_3$, δ): 159.86, 139.94, 136.46, 133.59, 131.72, 126.14, 122.72, 114.11, 113.21, 112.12, 43.60, 39.12, 34.69, 32.54, 31.93, 29.68, 29.65, 29.62, 29.59, 29.39, 29.37, 28.83, 27.44, 27.09, 25.68, 23.15, 22.70, 14.18, 14.14, 11.07. MS(MALDI-TOF): m/z calcd. for $C_{60}H_{92}N_2O_2S_2Br_2$ 1094.48, found 1093.505 $[M]^+$.

Synthesis of poly {3-(4,8-bis(5-(2-ethylhexyl)thiophen-2-yl)benzo[1,2-b:4,5-b']dithiophen-2-yl)-1,6-didodecylpyrido[2,3-g]quinoline-2,7(1*H*,6*H*)-dione} (PPQD-BDT): **M1** (0.21 g, 0.30 mmol), **M3** (0.27 g, 0.30 mmol), and tetrakis(triphenylphosphine)palladium(0) (10.3 mg, 8.92 μmol) were added into a 50-mL round-bottom flask. After sealing and purging with argon, chlorobenzene (CB; 4 mL) and DMF (1 mL) were added. The polymerization reaction mixture was stirred at 110 ℃ for 24 h. The polymer was end-capped by adding 0.1 equivalent of 2-(tributylstannyl)thiophene and 2-bromothiophene, followed by reaction for 1 h at 110 ℃. The crude product was precipitated in methanol (200 mL) and purified by Soxhlet extraction with acetone, hexane, and chloroform sequentially. The portion dissolved in chloroform was concentrated under reduced pressure and precipitated in methanol. The polymer was dried in a vacuum oven for 24 h to obtain 0.32 g product.

Synthesis of poly {3-(5-(4,8-bis(5-(2-ethylhexyl)thiophen-2-yl)benzo[1,2-b:4,5-b']dithiophen-2-yl)-4-(2-ethylhexyl)thiophen-2-yl)-1,6-didodecyl-8-(4-(2-ethylhexyl)thiophen-2-yl)pyrido[2,3-g]quinoline-2,7(1*H*,6H)-dione} (PPQDT-BDT): PPQDT-BDT was prepared using a procedure similar to that of PPQD-BDT. Specifically, **M2** (0.26 g, 0.24 mmol), **M3** (0.21 g, 0.24 mmol), and tetrakis(triphenylphosphine)palladium(0) (8.23 mg, 7.12 μmol) were added to a 50-mL round-bottom flask. After sealing and purging with argon, **M1** and **M3** were copolymerized. Yield: 0.27 g.

Results and Discussion

Synthetic routes of the PQD derivatives **M1** and **M2** and the corresponding copolymers are depicted in Scheme 1 and 2,

respectively. The detailed synthetic methods are described above in the Experimental section.

Compound **6**, a PQD building block, was synthesized via Pd-catalyzed Heck cross-coupling and ring-closing reactions. The monomer **M1** was successfully synthesized via further bromination with bromine and iron (III) chloride. Compound **7** was prepared by the Stille coupling reaction between **M1** and tributyl(4-(2-ethylhexyl)thiophen-2-yl)stannane, and finally the monomer **M2** was synthesized by bromination of **7**. Two new copolymers, PPQD-BDT and PPQDT-BDT, were synthesized by the Stille cross-coupling polymerization of the BDT derivative **M3** and monomer **M1** or **M2**. These copolymers showed moderate solubility in common organic solvents including chloroform, CB, and *o*-dichlorobenzene. PPQDT-BDT had a number-average molecular weight (M_n) of 22000 g mol^{-1} and a polydispersity index (PDI, $Đ$) of 4.06, whereas the respective values for PPQD-BDT were 12000 g mol^{-1} and 4.21, as measured using gel permeation chromatography (GPC) with chloroform as an eluent at 35 ℃.

Thermal properties of the two copolymers were investigated using TGA and DSC. Both copolymers showed good thermal stability with the decomposition temperatures (T_d, 5% weight loss) of 366 and 385 ℃ for PPQD-BDT and PPQDT-BDT, respectively. Their DSC thermograms displayed no thermal transition peaks between 30 and 300 ℃, as shown in Figure 1. These results indicate that the two copolymers should have adequate thermal stability for the fabrication of OPV devices.

To optimize the geometry of the polymer backbone, density functional theory (DFT) calculations were carried out in Gaussian 09W using Becke's three-parameter hybrid functional with the Lee-Yang-Parr correlation (B3LYP) and 6-31G(d) basis set. To simplify the calculations, the two polymers were simplified as dimer structures, and dodecyl chains on the lactam group and 2-ethylhexyl branched chains on the thiophene units were replaced by methyl and 2-methyl-propyl chains, respectively. In Figure 2, PPQD-BDT shows a low dihedral angle between the BDT unit and the PQD unit ($\theta = 8.9°$). PPQDT-BDT showed a slightly higher dihedral angle between the BDT unit and the thiophene unit ($\theta = 35.6°$), despite the low dihedral angle between the PQD unit and the thiophene unit ($\theta = 6.5°$). These facts indicate that PPQD-BDT has higher planarity than PPQDT-BDT. As expected, the FMO energy levels of the PPQDT-BDT model were higher than those of the PPQD-BDT model, owing to the thiophene spacer between the PQD and BDT building blocks in the former.[22] Specifically, the lowest unoccupied molecular orbital energy (E_{LUMO}) and the highest occupied molecular orbital energy (E_{HOMO}) of the PPQDT-BDT model were calculated as -2.61 and -4.78 eV, whereas the PPQD-BDT model had E_{LUMO} and E_{HOMO} as -2.70 and -4.84 eV, respectively.

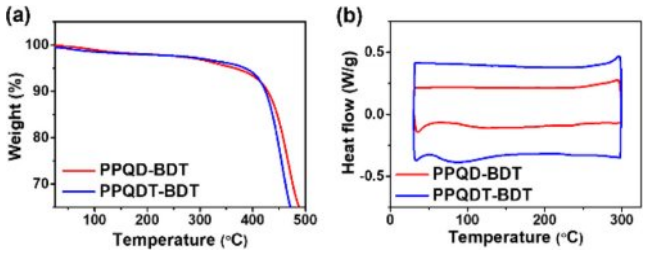

Figure 1. (a) TGA curves; (b) DSC thermograms of the synthesized copolymers.

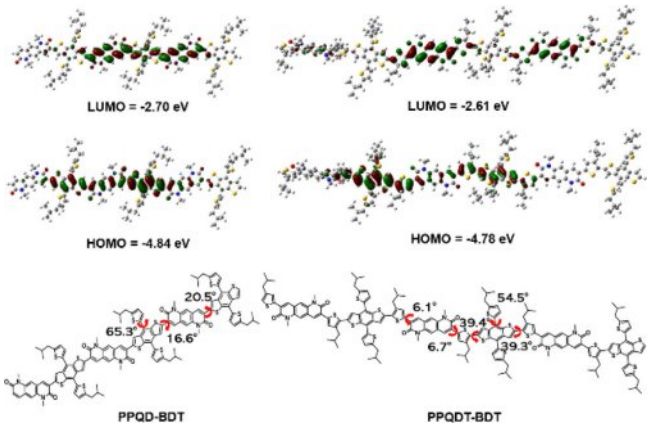

Figure 2. Minimum energy conformations and frontier molecular orbitals of the simplified PPQD-BDT and PPQDT-BDT trimer models with calculated torsional angles.

To investigate the optical properties of synthesized copolymers, UV-Vis absorption spectra were measured in the solution and thin-film states (Figure 3(a), (b), and Table 1). Both copolymers showed a broad absorption range from 300 to 700 nm, making them suitable donor materials for non-fullerene OSC. In both the solution and film states, PPQD-BDT exhibited the same absorption maximum (545 nm) and a shoulder peak at the longer wavelength side of this absorption maximum. This indicates that PPQD-BDT has strong intermolecular π–π stacking even in the solution state because of its planar polymer backbone, as can be seen from the DFT calculation results.[23] PPQDT-BDT showed absorption maxima at 557 and 572 nm in the solution and film states, respectively.[24] These maxima are red-shifted compared to PPQD-BDT due to the longer π-conjugation length after introducing a thiophene spacer between the BDT and PQD units. The optical bandgap (E_g^{opt}) of the copolymers was estimated to be 1.93 eV for PPQD-BDT and 1.85 eV for

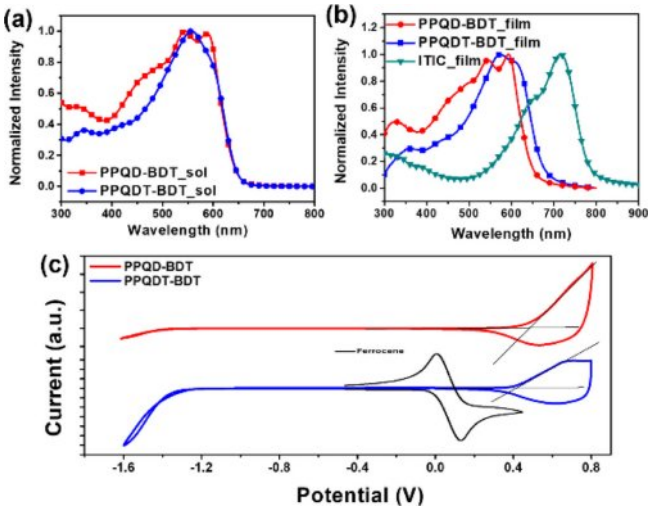

Figure 3. UV-Vis spectra of the synthesized copolymers in (a) solution; (b) film states; (c) Cyclic voltammograms of the two copolymers.

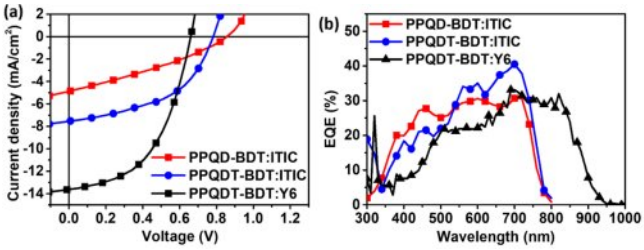

Figure 4. (a) *J-V* curves; (b) EQE spectra of OPV devices based on the synthesized copolymers.

PPQDT-BDT according to their absorption edge in the film state.

CV was performed to estimate the electrochemical properties of each polymer. From the results in Figure 3(c), PPQD-BDT and PPQDT-BDT had E_{HOMO} = -5.37 and -5.11 eV, respectively. PPQDT-BDT exhibited a higher E_{HOMO} than PPQD-BDT because of the electron-donating thiophene spacers on the polymer backbone.[25] E_{LUMO} was calculated to be -3.44 and -3.26 eV for PPQD-BDT and PPQDT-BDT, respectively, based on the equation $[E_{LUMO}]=[E_{HOMO}]+[E_g^{opt}]$.[26]

To evaluate the photovoltaic performance of the synthesized copolymers, inverted-architecture OPV devices were fabricated with the structure of indium tin oxide (ITO)/ZnO/polymer:ITIC/MoO_3/Ag. The device fabrication conditions were optimized by commonly used methods such as adjusting the donor/acceptor (D/A) weight ratio, adding a processing additive solvent, changing the thickness of the active layer, and a pre-annealing process. The optimized performances and the corresponding *J-V* curves and EQE spectra are shown in Figure 4 and Table 2.

The OPV device showed the best performance under the conditions of a D:A blend ratio of 1.0:1.0 w/w in solvent (chlorobenzene (CB) or chloroform (CF)) with 0.5% of diphenyl ether (DPE) as a processing additive solvent. Using ITIC as the acceptor, the V_{OC} values for PPQD-BDT and PPQDT-BDT were 0.86 and 0.72 V, respectively. PPQDT-BDT showed a lower V_{OC} value than PPQD-BDT owing to its higher HOMO energy level. Nevertheless, PPQDT-BDT produced higher J_{SC} and *FF* than those of PPQD-BDT. As a result, PPQDT-BDT exhibited a higher device PCE than PPQD-BDT (2.86% *vs*. 1.29%). Additionally, PPQDT-BDT with Y6 as the acceptor, the V_{OC} was decreased to 0.67 V. The J_{SC} value was increased to 13.24 mA/cm^2. As a result, the device of PPQDT-BDT with Y6 exhibited a higher device PCE performance than ITIC acceptor (4.52% *vs*. 2.86%).

Table 1. Optical and Electrochemical Properties of the Synthesized Copolymers

	Solution	Film		E_g^{opt} (eV)[b]	E_{HOMO}^{CV} (eV)[c]	E_{LUMO}^{opt} (eV)[d]
	λ_{max} (nm)	λ_{max} (nm)[a]	λ_{edge} (nm)			
PPQD-BDT	545 (588)	545 (593)	644	1.93	-5.37	-3.44
PPQDT-BDT	557	572	672	1.85	-5.11	-3.26

[a]The value in the bracket is shoulder peak; [b]Calculated from the absorption λ_{edge} of polymer films : E_g = 1240 nm/λ_{edge}; [c]HOMO levels were measured by cyclic voltammetry : E_{HOMO} = -4.71-[V_{oxi}]; [d]LUMO levels were calculated from the HOMO and the corresponding optical bandgap. $E_{LUMO}=E_{HOMO}+E_g^{opt}$.

Table 2. Characteristics of OSC Devices Based on the Synthesized Copolymers

Polymer:Acceptor	V_{oc} (V)	J_{sc} (mA/cm^2)	J_{calc} (mA/cm^2)	FF	PCE (%)
PPQD-BDT:ITIC	0.85±0.01(0.86)	4.86±0.07(4.91)	6.67	31.04±1.06(32.07)	1.29±0.07(1.34)
PPQDT-BDT:ITIC	0.72±0.04(0.78)	7.70±0.20(7.89)	7.31	46.09±2.51(48.51)	2.57±0.21(2.86)
PPQDT-BDT:Y6	0.66±0.01(0.67)	12.45±0.84(13.62)	13.24	46.79±2.69(50.29)	3.84±0.48(4.52)

The values in the bracket are maximum parameters of the devices.

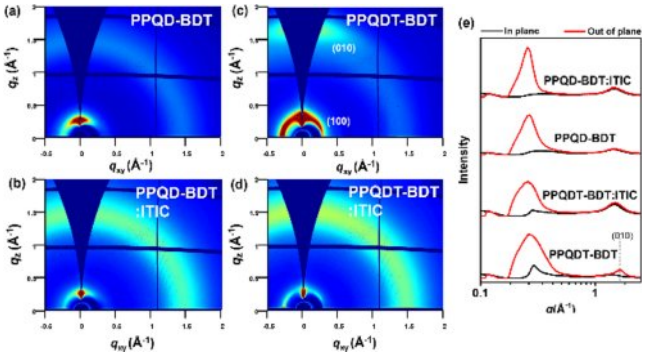

Figure 5. 2D-GIXD images of neat polymer films of (a) PPQD-BDT; (c) PPQDT-BDT as well as blend films; (b) PPQD-BDT:ITIC; (d) PPQDT-BDT:ITIC; (e) Line-cut profiles of neat polymer and blend films.

To analyze the device performance, grazing incidence wide-angle X-ray scattering (GIWAXS) measurements were performed to investigate the morphologies of the neat polymer and D-A blend films. Figure 5 shows the GIWAXS images and the corresponding in-plane (IP)/out-of-plane (OOP) line-cut profiles of the neat polymer and blend films. The neat PPQDT-BDT polymer film showed π–π stacking diffraction in OOP at 1.66 Å^{-1} with a corresponding distance of 3.79 Å, as well as lamellar repeating located at 0.29 Å^{-1} in IP with a corresponding distance of 21.66 Å. In contrast, the neat PPQD-BDT polymer film showed an isotropic orientation, and so did both polymer blend films with a non-fullerene acceptor, ITIC. The collapsed orientation in the blend films results in charge recombination at the donor-acceptor interface, leading to overall low J_{SC} and FF values of the OPV devices.[27] Atomic force microscopy (AFM) analysis was performed to further investigate the film morphology. Figure 6 shows AFM images of the polymer:ITIC blend films as both phase images (a, c) and height images (b, d). The two blend films showed phase-separated morphology with a moderate root-mean square (RMS, R_q) of 4.20 and 4.98 nm for PPQD-BDT and PPQDT-BDT, respectively. Both copolymer blend films exhibited phase separation between the polymer and ITIC, and this self-aggregation led to unfavorable charge dissociation and charge recombination, resulting in an inferior PCE with low J_{SC} and *FF*.[28,29] These weak molecular orientations and separated morphologies in the D-A blend films of PPQD-BDT and PPQDT-BDT affected the OPV devices and resulted in moderate device performance. It is believed that PPQDT-BDT delivered better device performance due to its relatively better crystallinity than PPQD-BDT, according to the UV-Vis absorption and GIWAXS data.

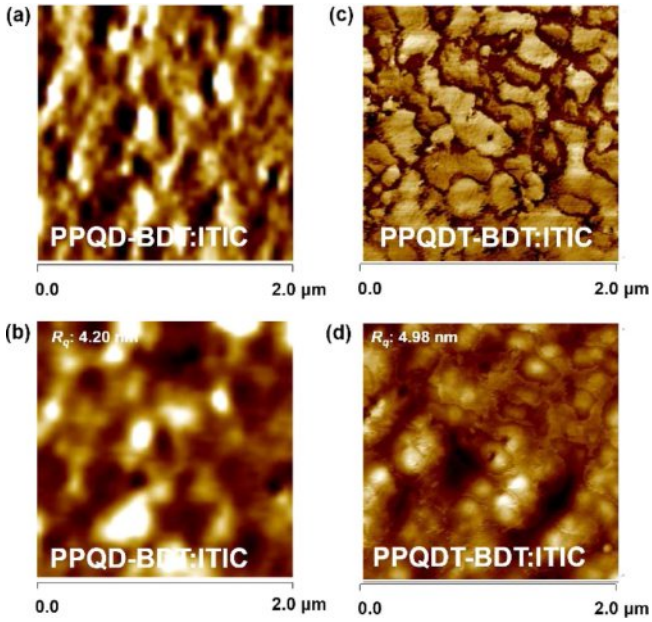

Figure 6. Tapping-mode AFM images (2 μm × 2 μm) of (a, b) PPQD-BDT:ITIC; (c, d) PPQDT-BDT:ITIC; (a, c) are the phase images; (b, d) are the height images.

Conclusions

In summary, a new polycyclic lactam structure, pyrido[2,3-*g*]quinoline-2,7(1*H*,6*H*)-dione (PQD), was designed as an electron-withdrawing building block for the polymer donor materials in OPVs. Two new copolymers, PPQD-BDT and PPQDT-BDT were further synthesized by incorporating BDT and PQD units using systematic design rules of alternating donor and acceptor units. The synthesized copolymers showed a broad absorption range between 300 and 700 nm and sufficiently high thermal stability for fabricating OPV devices. One of the fabricated OSC devices with PPQDT-BDT:Y6 blending achieved maximum PCE of 4.52%. Although these two copolymers did not realize remarkable performance in the fabricated OPV devices, the newly synthesized PQD building block is expected to be usefully applied to various organic semiconductor molecules or polymers for diverse electronic devices.

Acknowledgments. This work was supported by a 2-Year research grant from Pusan National University.

References

1. Kang, H.; Kim, G.; Kim, J.; Kwon, S.; Kim, H.; Lee, K. Bulk-Heterojunction Organic Solar Cells: Five Core Technologies for Their Commercialization. *Adv. Mater.* **2016**, 28, 7821-7861.
2. Søndergaard, R.; Hösel, M.; Angmo, D.; Larsen-Olsen, T. T.; Krebs,

F. C. Roll-to-roll Fabrication of Polymer Solar Cells. *Mater. Today*, **2012**, 15, 36-49.
3. Dai, S.; Zhan, X. Nonfullerene Acceptors for Semitransparent Organic Solar Cells. *Adv. Energy Mater.* **2018**, 8, 1800002.
4. Kaltenbrunner, M.; White, M. S.; Głowacki, E.D.; Sekitani, T.; Someya, T.; Sariciftci, N. S.; Bauer, S. Ultrathin and Lightweight Organic Solar Cells with High Flexibility. *Nat. Commun.* **2012**, 3, 770.
5. Upama, M. B.; Wright, M.; Elumalai, N. K.; Mahmud, M. A.; Wang, D.; Xu, C.; Uddin, A. High-Efficiency Semitransparent Organic Solar Cells with Non-Fullerene Acceptor for Window Application. *ACS Photonics*, **2017**, 4, 2327-2334.
6. Ha, J.-W.; Jung, J. G.; Ryu, D. H.; Lee, S.; Song, C. E.; Lim, B.; Jung, Y. J.; Park, J. M.; Hwang, D.-H. Thienoquinolinone-based Acceptor-π-acceptor-type Building Block for Polymer Donors in Organic Solar Cells. *Macromol. Res.* **2023**, 31, 25-31.
7. Cui, Y.; Xu, Y.; Yao, H.; Bi, P.; Hong, L.; Zhang, J.; Zu, Y.; Zhang, T.; Qin, J.; Ren, J.; Chen, Z.; He, C.; Hao, X.; Wei, Z.; Hou, J. Single-Junction Organic Photovoltaic Cell with 19% Efficiency. *Adv. Mater.* **2021**, 33, 2102420.
8. Cui, Y.; Yao, H.; Zhang, J.; Xian, K.; Zhang, T.; Hong, L.; Wang, Y.; Xu, Y.; Ma, K.; An, C.; He, C.; Wei, Z.; Gao, F.; Hou, J. Single-Junction Organic Photovoltaic Cells with Approaching 18% Efficiency. *Adv. Mater.* **2020**, 32, 1908205.
9. Park, J.; Chetan, L.; Kim, H.; Jee, J.-S.; Gal, Y.-S.; Jin, S.-H. New Pyrazine-based π-conjugated Polymer for Dopant-free Perovskite Solar Cell. *Macromol. Res.* **2024**, 32, 505-513.
10. Scharber, M. C.; Mühlbacher, D.; Koppe, M.; Denk, P.; Waldauf, C.; Heeger, A. J.; Brabec, C. J. Design Rules for Donors in Bulk-Heterojunction Solar Cells—Towards 10% Energy-Conversion Efficiency. *Adv. Mater.* **2006**, 18, 789-794.
11. Xu, T.; Yu, L. How to Design Low Bandgap Polymers for Highly Efficient Organic Solar Cells. *Mater. Today*, **2014**, 17, 11-15.
12. Sun, C.; Pan, F.; Qiu, B.; Qin, S.; Chen, S.; Shang, Z.; Meng, L.; Yang, C.; Li, Y. D–A Copolymer Donor Based on Bithienyl Benzodithiophene D-Unit and Monoalkoxy Bifluoroquinoxaline A-Unit for High-Performance Polymer Solar Cells. *Chem. Mater.* **2020**, 32, 3254-3261.
13. Hfaiedh, A.; Labiedh, M.; Mabrouk, A.; Braiek, M. B.; Alimi, K. Synthesis, Characterization and Structure–property Study of New Push–pull Carbazole Materials. *Macromol. Res.* **2023**, 31, 981-999.
14. Park, J. S.; Kim, G. U.; Lee, D.; Lee, S.; Ma, B.; Cho, S.; Kim, B. J. Importance of Optimal Crystallinity and Hole Mobility of BDT-Based Polymer Donor for Simultaneous Enhancements of V_{oc}, J_{sc}, and FF in Efficient Nonfullerene Organic Solar Cells. *Adv. Funct. Mater.* **2020**, 30, 2005787.
15. Zheng, B.; Huo, L.; Li, Y. Benzodithiophenedione-based Polymers: Recent Advances in Organic Photovoltaics. *NPG Asia Mater.* **2020**, 12, 3.
16. Yao, H.; Ye, L.; Zhang, H.; Li, S.; Zhang, S.; Hou, J. Molecular Design of Benzodithiophene-Based Organic Photovoltaic Materials. *Chem. Rev.* **2016**, 116, 7397-7457.
17. Jung, E. H.; Ahn, H.; Jo, W. H.; Jo, J. W.; Jung, J. W. Isoindigo-Based Conjugated Polymer for High-performance Organic Solar Cell with a High V_{OC} of 1.06 V as Processed from Non-halogenated Solvent. *Dyes Pigm.* **2019**, 161, 113-118.
18. Aumaitre, C.; Morin, J. F. Polycyclic Aromatic Hydrocarbons as Potential Building Blocks for Organic Solar Cells. *Chem Rec.* **2019**, 19, 1142-1154.
19. Zhao, C.; Guo, Y.; Zhang, Y.; Yan, N.; You, S.; Li, W. Diketopyrrolopyrrole-based Conjugated Materials for Non-fullerene Organic Solar Cells. *J. Mater. Chem. A*, **2019**, 7, 10174-10199.
20. Zhou, Y.; Zhang, W.; Yu, G. Recent Structural Evolution of Lactam- and Imide-functionalized Polymers Applied in Organic Field-effect Transistors and Organic Solar Cells. *Chem. Sci.* **2021**, 12, 6844-6878.
21. Yoon, W. S.; Kim, D. W.; Park, J.-M.; Cho, I.; Kwon, O. K.; Whang, D. R.; Kim, J. H.; Park, J.-H.; Park, S. Y. A Novel Bis-Lactam Acceptor with Outstanding Molar Extinction Coefficient and Structural Planarity for Donor–Acceptor Type Conjugated Polymer. *Macromolecules* **2016**, 49, 8489-8497.
22. Choi, M.-H.; Song, K.W.; Moon, D.K. Alkylidenefluorene–isoindigo Copolymers with An Optimized Molecular Conformation for Spacer Manipulation, π–π Stacking and Their Application in Efficient Photovoltaic Devices. *Polym. Chem.* **2015**, 6, 2636-2646.
23. Liu, H.-H.; Chang, S.-L.; Huang, K.-H.; Cao, F.-Y.; Cheng, K.-Y.; Sun, H.-S.; Lai, Y.-Y.; Cheng, Y.-J. Two-Dimensional Tetrathienonaphthalenes-Based Donor–Acceptor Copolymers: Synthesis, Isomeric Effect, and Organic Field-Effect Transistors. *Macromolecules* **2020**, 53, 7740-7748.
24. Kan, B.; Chen, X.; Gao, K.; Zhang, M.; Lin, F.; Peng, X.; Liu, F.; Jen, A.K.-Y. Asymmetrical Side-chain Engineering of Small-molecule Acceptors Enable High-performance Nonfullerene Organic Solar Cells. *Nano Energy*, **2020**, 67, 104209.
25. Xiao, Z.; Subbiah, J.; Sun, K.; Ji, S.; Jones, D. J.; Holmes, A. B.; Wong, W. W. H. J. Mater. Thiazolyl Substituted Benzodithiophene Copolymers: Synthesis, Properties and Photovoltaic Applications. *Chem. C*, **2014**, 2, 1306-1313.
26. Leounat, L.; Sbarcea, G.; Branzoi, I. V. Cyclic Voltammetry for Energy Levels Estimation of Organic Materials. *Sci. Bull. Series B*, **2013**, 75, 111-118.
27. Tumbleston, J.R.; Collins, B.A.; Yang, L.; Stuart, A.C.; Gann, E.; Ma, W.; You, W.; Ade, H. The Influence of Molecular Orientation on Organic Bulk Heterojunction Solar Cells. *Nat. Photonics*, **2014**, 8, 385-391.
28. Caballero-Quintana, I.; Amargos-Reyes, O.; Maldonado, J. L.; Nicasio-Collazo, J.; Romero-Borja, D.; Barreiro-Arguelles, D.; Molnar, G.; Bousseksou, A. Scanning Probe Microscopy Analysis of Nonfullerene Organic Solar Cells. *ACS Appl. Mater. Interfaces* **2020**, 12, 29520-29527.
29. Li, W.; Chen, M.; Cai, J.; Spooner, E. L. K.; Zhang, H.; Gurney, R. S.; Liu, D.; Xiao, Z.; Lidzey, D. G.; Ding, L.; Wang, T. Molecular Order Control of Non-fullerene Acceptors for High-Efficiency Polymer Solar Cells. *Joule*, **2019**, 3, 819-833.